Polímeros
ISSN 1678-5169 (Online)

https://doi.org/10.1590/0104-1428.20210097

ORIGINAL ARTICLE

Development and characterization of green polyethylene/clay/antimicrobial additive nanocomposites[a]

Priscylla Jordânia Pereira de Mesquita[1], Tatianny Soares Alves[2] and Renata Barbosa[2]*

[1]Laboratório de Polímeros e Materiais Conjugados, Pós-graduação em Ciência e Engenharia dos Materiais, Centro de Tecnologia, Universidade Federal do Piauí – UFPI, Teresina, PI, Brasil

[2]Laboratório de Polímeros e Materiais Conjugados, Curso de Engenharia de Materiais, Centro de Tecnologia, Universidade Federal do Piauí – UFPI, Teresina, PI, Brasil

[a]This paper has been partially presented at the 16th Brazilian Polymer Congress, held on-line, 24-28/Oct/2021

**rrenatabarbosa@yahoo.com*

Abstract

In this work, nanocomposites were developed and evaluated using high-density bio polyethylene (BPEAD)/Cloisite 20A (3 and 6%)/commercial antimicrobial additive (0,5 and 1%) containing 1% of zinc pyrithione dispersed in vinyl acetate (EVA). The samples were prepared in a single screw extruder using the melt intercalation technique and then by flat extrusion to obtain the films. X-ray diffraction (XRD) showed an increase in basal spacing and exfoliation of the structure of some films. The Fourier Transform Infrared Spectroscopy (FTIR) analysis illustrated the main functional groups for BHDPE and EVA. Thermal analysis indicated that BHDPE degradation did not change with organoclay addition, but crystallinity increased. The mechanical properties showed an increase in the elastic modulus and a decrease in maximum tensile strength. This work contributes to the development and improvement of the natural properties of BHDPE in order to enlarge its applications.

Keywords: *bio polyethylene, clay, flat films, nanocomposites.*

How to cite: Mesquita, P. J. P., Alves, T. S., & Barbosa, R. (2022). Development and characterization of green polyethylene/clay/antimicrobial additive nanocomposites. *Polímeros: Ciência e Tecnologia*, *32*(2), e2022022. https://doi.org/10.1590/0104-1428.20210097

1. Introduction

Biopolymers and their innovative technological processes have been studied in several applications. As known, primarily for their environmental benefits, biopolymers are considered promising alternatives to petroleum-based polymers, as most can help reduce environmental pollution and greenhouse gas emissions[1,2].

Although the term "biopolymer" has several different definitions depending on the area involved, the most widely accepted one relates biopolymers to biobased and biodegradable materials. According to the IUPAC (International Union of Pure and Applied Chemistry), biologically-based polymers are derived from biomass or produced from monomers from its derivation. Hence, green polyethylene is an example of bio-based polymers[3,4].

Green polyethylene or bio polyethylene is produced from sugarcane ethanol, converted to ethylene via dehydration. According to life cycle assessment studies, bio polyethylene has a smaller carbon footprint than petroleum-based polyethylene. Furthermore, it has the differential of capturing carbon dioxide during its production, contributing to reducing greenhouse gas emissions, and maintaining the same properties, performance, and versatility of the conventional resin, which facilitates its application in the chains of existing production and recycling[5-7].

Biopolymers have a lot of potentials. Despite increasing production capacity, they are still quite expensive, arousing interest in modification processes such as blending with other polymers and adding plasticizers or fillers[8].

The use of polymer/clay nanocomposites has been intensively studied in recent years, mainly due to improvements in mechanical, thermal, and barrier properties[9-12]. In this work, montmorillonite organophilic clay is used to produce nanocomposites. The packaging sector has invested in developing these nanocomposites, as the nanoclay, when dispersed in the polymer matrix, results in a homogeneous layer, creating tortuous paths, making it difficult for molecules to diffuse throughout the matrix[13,14].

The homogeneous dispersion of nanoclay in an organic polymer is not easily achieved due to the hydrophilicity of the clay, so the clays are organically modified to increase the affinity between the clay and the polymer, also growing the interlayer distance and lipophilicity of the nanoclay[15]. This behavior was reported in studies with nanometric clay to polyethylene. In this case, the authors used montmorillonite

in proportions of 3 to 5% in the polyethylene matrix to form nanocomposites and obtained improvements in mechanical and thermal properties[16]. In another study, the researchers added montmorillonite clay in 0.5 to 2.5% fractions and acquired better mechanical properties when incorporating it into the blend composed of polyethylene and polyamide[17].

Compatibilizing agents are also used to improve the intercalation of nanocomposites by increasing the interlayer distance of the nanoclays[18]; they may also contain biocidal groups incorporated in the polymer structure, thus conferring an antimicrobial character[19]. Chemically, antimicrobial additives can be classified by their active components. In this work, zinc pyrithione dispersed in a Vinyl Acetate (EVA) matrix was used. In addition to having antimicrobial activity against fungi, bacteria, and algae, this coordination compound has a melting point at 240 °C and can be processed with most thermoplastics and elastomers[20].

In this context, packaging has reinvented itself with more attractive features, the so-called smart or active packaging. Active packaging is a system that combines the benefits of measuring, estimating, or predicting different aspects of food quality or safety with the release of an active substance that extends the shelf life of the product[21]. Among active packaging, antimicrobial packaging becomes an up-and-coming type as it provides for the addition of an extra barrier (microbiological) to physical barriers (oxygen and moisture)[22].

Many studies with PE and its composites have been dedicated to the development of antimicrobial packaging, as in studies[23] that incorporated zinc oxide nanoparticles (ZnO-NPs) in low-density polyethylene and in studies[24] that incorporated ZnO-NPs in high-density polyethylene.

Faced with many opportunities, this study aimed to produce nanocomposites of high-density bio polyethylene (BHDPE), organophilic clay, and a commercial additive containing 1% of zinc pyrithione dispersed in vinyl acetate (EVA), which was used in the ratios of 0.5 and 1%. The films were produced in an extruder by the intercalation technique in the molten state with coupling to a matrix for flat films. The films were characterized by X-ray diffraction (XRD), Fourier Transform Infrared Spectroscopy (FTIR), Thermogravimetry (TG), Differential Scanning Calorimetry (DSC), and Tensile Strength Testing.

2. Materials and Methods

2.1 Materials

High-Density Bio polyethylene (BHDPE, SGM9450F), MFI = 9.3 g/10min, ASTM 1238 at 190 ºC, was supplied by BRASKEM's Petrochemical Complex in Triunfo (Brazil) and used as received. The filler incorporated into the BHDPE matrix was Cloisite 20A supplied by Southern Clay Products. The antimicrobial additive used was Sanitized MB E 22-70 provided by Clariant. The active compound used was zinc pyrionate dispersed in a vinyl acetate matrix.

2.2 Preparation of nanocomposite films

The samples were prepared using EVA BHDPE/Clay/Masterbatch containing zinc pyrithione, according to the proportions described in Table 1.

The mixtures of BHDPE, organophilic clay, and the antimicrobial additive were extruded in a single screw extruder (L/D = 26), model AX-16 from AX Plásticos, operating with temperatures ranging from the first to the third zone, respectively, between 200 ºC, 205 ºC, and 210 °C and screw speed at 50 rpm, conditions established in the laboratory.

After incorporating the additives into the polymer matrix, the films were prepared in a single-screw extruder with a flat die of 220 mm width and cylindrical cooling rollers, model Lab 16 from AX Plásticos, with a temperature profile of 205 °C, 210°C, and 180 °C and screw speed of 60 rpm. The thickness of the films was determined using a thickness gauge, and the averages found for five (5) samples were: 0.06 mm (BHDPE), 0.12 mm (N31), 0.11 mm (N32), 0.22 mm (N61), and 0.15 mm (N62).

2.3 Characterization of nanocomposite films

2.3.1 X-ray diffraction

The nanocomposites were analyzed by the X-ray diffraction (XRD) method in a Shimadzu model XRD 6000 diffractometer operating in the angular range (2θ) of 1.5 ° to 30° using CuKα as incident radiation was used to determine the crystalline parameters of the films.

2.3.2 Fourier Transform Infrared Spectroscopy (FTIR)

Fourier transform infrared spectroscopy (FTIR) analyses were performed on a Perkin Elmer SPECTRUM 400 (FT-IR/FT-NIR) spectrometer scanning from 4000 to 650 cm^{-1}.

2.3.3 Thermal analysis

The thermal properties of the samples were analyzed by thermogravimetry (TG), and differential scanning calorimetry (DSC) techniques in a TA Instrument a TA Instrument SDT Q600 V20.9 Build 20, operating at a heating rate of 10 °C/min, from ambient temperature to 600 °C, under 100 mL/min nitrogen gas flow. The degree of crystallinity (Xc) was calculated according to Equation 1, where ΔH_{of} is the melt enthalpy of an ideal polyethylene with 100% crystalline HDPE (289 J/g[24]) and ΔH_f is the melt enthalpy of the nanocomposites. The (x) values were adequate for the matrix weight fraction in the nanocomposites.

$$Xc = \frac{\Delta H_f * 100}{\Delta H^\circ_f \cdot xHDPE} \quad (1)$$

Table 1. Sample concentrations.

Samples	Green HDPE	Clay	Antimicrobial
BHDPE	100%	-	-
N31	96.5%	3%	0.5%
N32	96%	3%	1%
N61	93.5%	6%	0.5%
N62	93%	6%	1%

Source: Personal archive.

2.3.4 Tensile test

Tensile properties of the nancomposites e films were determined according to ASTM D882-02[25] in a Shimadzu brand AGS-X mechanical testing machine with a speed of 20 mm/min and a load cell of 5 kN. Five test specimens were used for each composition with dimensions of 120 mm in length and 25 mm in width.

3. Results and Discussion

3.1 X-Ray Diffraction (XRD)

The diffractograms illustrated in Figure 1 show the peaks of Cloisite 20A, BHDPE, and nanocomposites containing the antimicrobial additive and clay. For the BHDPE, a non-crystalline halo and a very intense peak between the 15° and 25° angles and other less severe peaks between the 26° and 40° angles were observed. As well, three crystalline peaks at 2θ = 21.55°, 23.89°, and 36.36° which are characteristic of the (110), (200) and (020) planes, respectively, in a crystalline region of polyethylene[25].

The diffractograms of BHDPE and nanocomposites illustrate similar behavior and sharpness in the characteristic peaks of BHDPE. It is observed the peaks of the clay Cloisite 20A at 2θ correspond to the (001) plane and basal interplanar distance of 3,4 nm[26]. It can be seen that the nanocomposites showed an increase in the basal interplanar distance of the peak corresponding to organophilic clay for the nanocomposite with the highest content of clay and antimicrobial agent.

This same behavior was reported[27] in studies using HDPE/montmorillonite/zinc oxide nanocomposite, observing an increase in the spacing between the clay layers with the addition of zinc oxide and HDPE.

3.2 Fourier Transform Infrared Spectroscopy (FTIR)

Figure 2 illustrates the infrared spectra for nanocomposite films with clay and the antimicrobial additive additions. The characteristic bands of polyethylene, 2918, 2849, 1469, 1463, 731 and 720 cm^{-1} (CH_2 angular deformations) appear in all spectra[28,29]. Studies[30] with nanocomposites using modified vermiculite with Zn^{2+} particles in the HDPE matrix also observed the same characteristic bands of pure HDPE.

The bands of the antimicrobial additive, composed of EVA[28,31], were not detected, suggesting an overlapping of the BHDPE bands due to the low concentration. However, the presence of bands in the range of 3620 cm^{-1} indicates the presence of O-H vibrations for Al-OH and Si-OH, and in approximately 1042 cm^{-1} the absorption of the Si-O from to Cloisite 20A[32]. In studies with nanocomposites using modified vermiculite with Zn^{2+} particles in HDPE matrix, bands ranging from 1007 to 1041 cm^{-1} were observed, corresponding to the stretching of Si-O of vermiculite, as well as an increase in the intensity of these bands with an increasing amount (3, 6 and 10% by weight) of the modified clay[30].

3.3 Thermogravimetry (TG)

Figure 3 illustrates the TG and DTG curves for BHDPE, Cloisite 20A, and nanocomposites. The BHDPE showed a single stage degradation, starting at 454°C and losing up to 50% of its mass at 482°C, having a degradation peak at 489°C, as shown in Table 2. Similar results were found by authors who analyzed the thermal behavior of polyethylene[33,34].

Cloisite 20A shows three degradation phases: first, dehydration before 150°C; then, decomposition of organic molecules between 200 and 500°C; and finally, dehydroxylation of aluminosilicate groups between 500 and 700°C[35,36].

For nanocomposites N32, N61, and N62, minor variations were observed in the degradation temperature with 10% and 50% mass loss. However, for N31, a 10ºC decrease in degradation temperature was observed at 50% mass loss as shown in the data reported in Table 2. Studies[37] with EVA and silicates showed that the degree of clay dispersion affects matrix degradation and deacetylation of EVA, promoting an acceleration of degradation.

Organophilic clay has two opposite functions in the thermal stability of polymer/clay nanocomposites: barrier and catalysis effects. The first improves thermal stability while the second accelerates degradation[33]. Another factor that leads to faster thermal degradation of the matrix is related

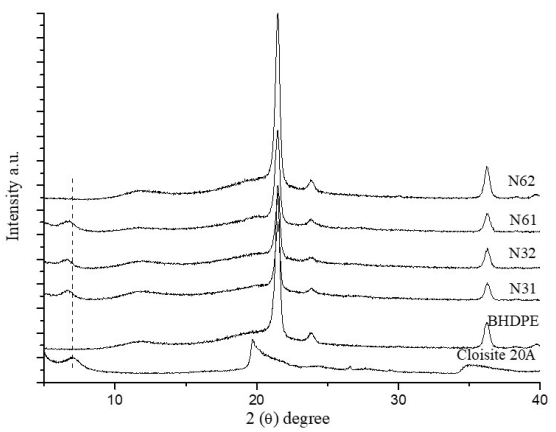

Figure 1. X-ray diffractograms of Cloisite 20A, BHDPE and nanocomposites.

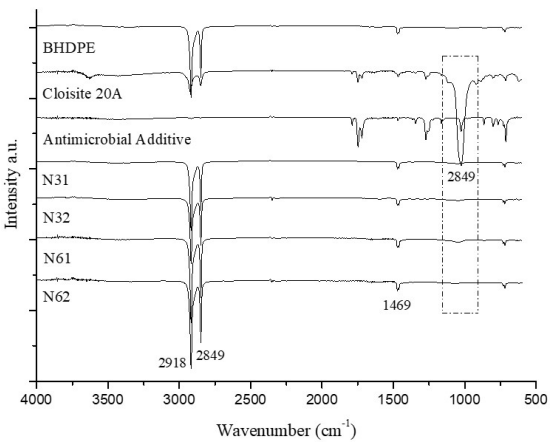

Figure 2. FTIR of the antimicrobial additive, BHDPE, N31, N32, N61, and N62.

Table 2. TG and DTG(derived thermogravimetry), BHDPE, Cloisite 20A and nanocomposites.

Samples	Temperature (°C) for mass loss		Tp (°C)	Residue at 500 °C/%
	10%	50%		
BHDPE	454	482	489	0.0
Cloisite 20A	299	-	312	72.23
N31	428	472	479	0.65
N32	453	481	481	2.74
N61	450	480	483	2.99
N62	453	484	489	4.93

Source: Personal archive.

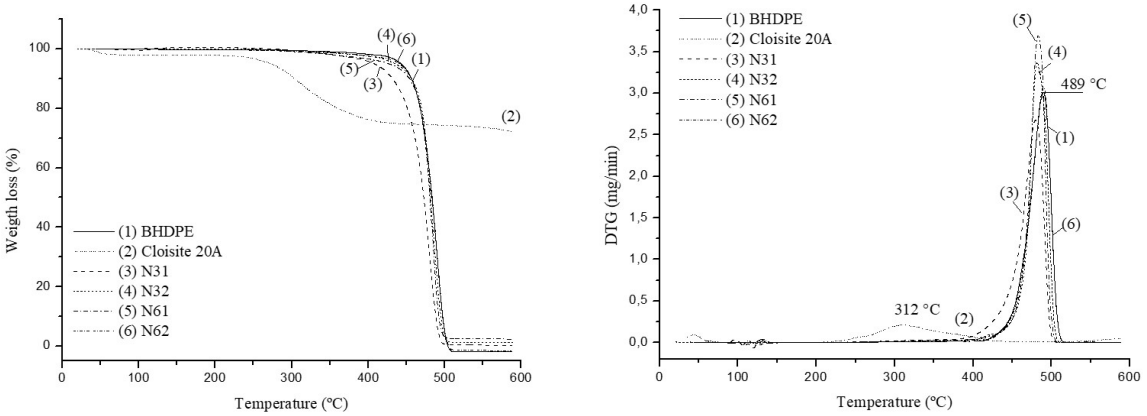

Figure 3. TG and DTG curves of BHDPE, Cloisite 20A and nanocomposites.

to the alkylammonium cations present in the organoclay that can undergo decomposition by Hoffmann reaction. Their decomposition products catalyze polymeric degradation. Therefore, when a low fraction of organoclay is added to the polymer matrix, the clay must be well dispersed for the barrier effect to be predominant[38,39]. For N62, better clay dispersion was observed, as shown by the XRD analysis, and consequently, better thermal stability than the others in which the catalytic effect prevailed. The observed residues may also be due to other fillers and carbonaceous products.

3.4 Differential Scanning Calorimetry (DSC)

DSC curves illustrate two essential parameters for the study of thermal stability: crystallinity and melting point. Figure 4 illustrates the DSC curves for BHDPE and its nanocomposites. BHDPE showed an endothermic peak at 139 °C related to its melting temperature, enthalpy of melting of 134.75 J/g, and crystallinity of 46.3%, according to Table 3. Similar results were found by authors who analyzed polyethylene by DSC[2,27].

The N32, N61, and N62 nanocomposites did not undergo significant variation in the melting temperature. However, N31 showed a 12 ºC decrease in this parameter compared to BHDPE, as shown in Table 3. Similar behavior was displayed by LDPE/Cloisite15A/EVA nanocomposites, where a decrease in melting temperature and crystallinity was observed[40].

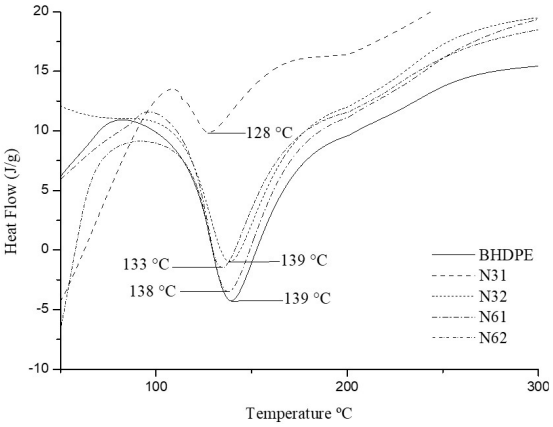

Figure 4. DSC curves for BHDPE, N31, N32, N61, N62.

In the analysis of Table 3, there is a slight decrease in the melting temperature for the nanocomposites. The addition of clay in N31 and N32 made nucleation difficult and decreased the degree of crystallinity. On the other hand, increasing the amount of clay led to increased crystallinity. The increase in the EVA content also led to higher degrees of crystallinity in the nanocomposites.

This effect corroborates the results presented in the literature[41-43], which indicate that nanofiller help accelerate the crystal growth, which leads to crystallization at higher

temperatures, but can also, as in this case, generate a structure with a lower degree of crystallinity, so that a more significant number of smaller crystals are obtained.

3.5 Mechanical properties

The tensile strength of BHDPE and nanocomposites are illustrated in Figure 5, in which BHDPE had a maximum tensile strength of 58.77 MPa and nanocomposites N31, N32 and N62 showed a decrease in strength, while N61 had an increase of 21%, these values are dependent on film thickness, load direction, and processing conditions. Among the nanocomposites, it is observed that the increase in clay and EVA favored the increase in strength.

In general, the addition of Cloisite 20A and the antimicrobial agent was expected to increase the tensile strength, as occurred in N61. However, the formation of agglomerates in the matrix can occur, causing defects that concentrate mechanical stress[42,43,44] and weak interaction between EVA/Clay as reported in studies based on PE, EVA, and zinc oxide nanoparticles[20].

Figure 6 illustrates the elastic modulus values for BHDPE and nanocomposites. BHDPE had a modulus of 1384.85 MPa, an increase in this property is observed for all nanocomposites compared to HDPE. N31 had a lower modulus compared to N32, although with similar thicknesses (0.12 and 0.11 mm, respectively). N61 had the highest modulus of elasticity and the most significant thickness (0.22 mm) compared to N62 (0.15 mm). In this case, it was not possible to observe a relationship between the increase in clay and antimicrobial with the increase in the modulus of elasticity.

The decrease in mechanical properties would be associated with the high mobility of the EVA phases, which accentuates the defects around the interfaces formed between the polymers and the nanoparticles agglomerates. This effect is accentuated due to the immiscibility between the nanoparticles and the polymer matrix. Because the polymers (PE and EVA) are hydrophobic and the inorganic nanoparticles are hydrophilic and, when mixed, form agglomerates that prevent the transfer of mechanical loads throughout the polymer matrix of the mixture[20].

The mechanical properties are listed in Table 4, noting that the yield strength follows the same behavior as the ultimate tensile strength, showing a decrease for N31, N32, and N62, while for N61, there was an increase. It is possible to observe that nanocomposites did not present great deformation compared to BHDPE, considering the applied stress and modulus of elasticity, confirming the behavior of increasing stiffness.

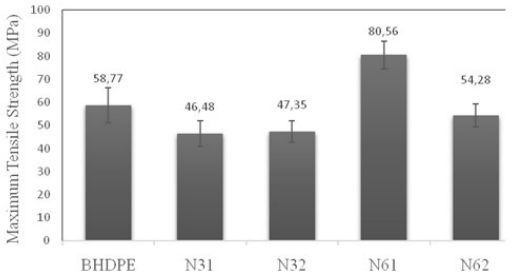

Figure 5. Maximum tensile strength of BHDPE and nanocomposites.

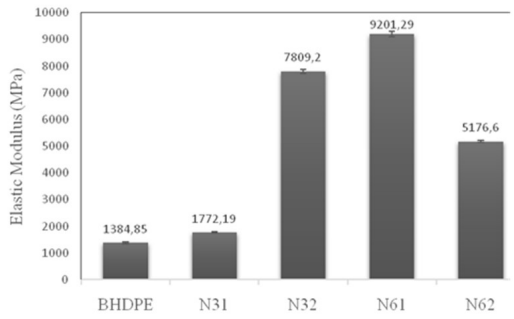

Figure 6. Elastic modulus of BHDPE and nanocomposites.

Table 3. DSC of BHDPE and nanocomposites.

Samples	Tm (°C)	ΔH_f (J/g)	Xc (%)
BHDPE	139	134.75	46.3
N31	128	90.47	31.9
N32	139	104.9	38.8
N61	138	136.5	49.8
N62	133	142.2	52.1

Source: Personal archive.

Table 4. Mechanical properties of BHDPE and nanocomposites.

Samples	Yield Stress (MPa)	Tensile Strength (MPa)	Strain at break (%)	Elastic Modulus (MPa)
BHDPE	58.16 ±7.1	58.77 ± 7.6	58.81 ± 4.1	1384.85 ± 38.6
N31	37.21 ± 4.4	46.48 ± 5.6	53.78 ± 3.2	1772.19 ± 34.8
N32	39.04 ± 4.5	47.35 ± 4.6	61.79 ± 5.4	7809.2 ± 75.6
N61	70.85 ± 10.7	80.56 ± 6.0	68.58 ± 6.5	9201.29 ± 101.2
N62	51.76 ± 3.8	54.28 ± 4.9	49.61 ± 3.7	5176.6 ± 45.5

Source: Personal archive.

4. Conclusions

The interest in the production of polymeric nanocomposites comes from the wide range of resulting properties and the possibility of varying additives and production processes. In this work, BHDPE/Cloisite20A/EVA nanocomposites were studied. Through XRD analysis, it can be verified that the nanocomposites showed an increase in the interplanar basal distance due to the incorporation of polymer chains in the clay lamellae. By FTIR, it was possible to observe the presence of clay in the spectra of the nanocomposites, not being possible to observe the characteristic bands of EVA, since the bands may have overlapped and also due to the very small amount of EVA in the system. The thermal behavior of nanocomposites was similar to that of BHDPE, with a reduction in degradation temperature and melting temperature only observed for N31, in which clay had a catalytic action. Thus, compared to BHDPE, nanocomposites did not have their thermal stability compromised. The inclusion of clay and EVA in the BHDPE matrix resulted in a decrease in yield stress and tensile strength limit for N31, N32, N62 and an increase for N61. As for the modulus of elasticity, there was an increase compared to BHDPE, but it was not possible to establish a relationship between an increase in clay and EVA and the increase in modulus. Therefore, it can be seen that BHDPE/Cloisite20A/EVA nanocomposites are promising since it is possible to maintain or improve some properties, conferring antimicrobial properties, it is necessary to deepen the study of the proportions of additives and interaction mechanisms between Clay/EVA.

5. Author's Contribution

- **Conceptualization** – Renata Barbosa; Tatianny Soares Alves.
- **Data curation** – Priscylla Jordânia Pereira de Mesquita.
- **Formal analysis** – Priscylla Jordânia Pereira de Mesquita.
- **Investigation** – Renata Barbosa; Tatianny Soares Alves; Priscylla Jordânia Pereira de Mesquita.
- **Methodology** – Priscylla Jordânia Pereira de Mesquita.
- **Project administration** – Renata Barbosa.
- **Resources** – Renata Barbosa; Tatianny Soares Alves.
- **Software** – Priscylla Jordânia Pereira de Mesquita.
- **Supervision** – Renata Barbosa; Tatianny Soares Alves.
- **Validation** – NA.
- **Visualization** – NA.
- **Writing – original draft** – Priscylla Jordânia Pereira de Mesquita.
- **Writing – review & editing** – Renata Barbosa; Tatianny Soares Alves.

6. Acknowledgements

The authors acknowledge the support from the Federal University of Piauí (UFPI), Piauí State Research Support Foundation (FAPEPI), National Council for Scientific and Technological Development (CNPq), and Funding: This work was supported by the CNPq [process number: 308446/2018-6].

7. References

1. Mehta, N., Cunningham, E., Roy, D., Cathcart, A., Dempster, M., Berry, E., & Smyth, B. M. (2021). Exploring perceptions of environmental professionals, plastic processors, students and consumers of bio-based plastics: informing the development of the sector. *Sustainable Production and Consumption*, *26*, 574-587. http://dx.doi.org/10.1016/j.spc.2020.12.015.
2. Mazur, K., Jakubowska, P., Romanska, P., & Kuciel, S. (2020). Green high-density polyethylene (HDPE) reinforced with basalt fiber and agricultural fillers for technical applications. *Composites. Part B, Engineering*, *202*, 108399. http://dx.doi.org/10.1016/j.compositesb.2020.108399.
3. Vert, M., Doi, Y., Hellwich, K.-H., Hess, M., Hodge, P., Kubisa, P., Rinaudo, M., & Schué, F. (2012). Terminology for biorelated polymers and applications (IUPAC Recommendations 2012). *Pure and Applied Chemistry*, *84*(2), 377-410. http://dx.doi.org/10.1351/PAC-REC-10-12-04.
4. Brodin, M., Vallejos, M., Opedal, M. T., Area, M. C., & Chinga-Carrasco, G. (2017). Lignocellulosics as sustainable resources for production of bioplastics – a review. *Journal of Cleaner Production*, *162*, 646-664. http://dx.doi.org/10.1016/j.jclepro.2017.05.209.
5. Dilkes-Hoffman, L., Ashworth, P., Laycock, B., Pratt, S., & Lant, P. (2019). Public attitudes towards bioplastics – knowledge, perception and end-of-life management. *Resources, Conservation and Recycling*, *151*, 104479. http://dx.doi.org/10.1016/j.resconrec.2019.104479.
6. Nagakawa, Y., Yunoki, S., & Saito, M. (2014). Liquid scintillation counting of solid-state plastic pellets to distinguish bio-based polyethylene. *Polymer Testing*, *33*, 13-15. http://dx.doi.org/10.1016/j.polymertesting.2013.10.018.
7. Santos, L. A. Jr., Thiré, R. M. S. M., Lima, E. M. B., Racca, L. M., & Silva, A. L. N. (2018). Mechanical and thermal properties of environment friendly composite based on mango's seed shell and high-density polyethylene. *Macromolecular Symposia*, *381*(1), 1800125. http://dx.doi.org/10.1002/masy.201800125.
8. Sionkowska, A. (2011). Current research on the blends of natural and synthetic polymers as new biomaterials. *Progress in Polymer Science*, *36*(9), 1254-1276. http://dx.doi.org/10.1016/j.progpolymsci.2011.05.003.
9. Chen, L., Rende, D., Schadler, L. S., & Ozisik, R. (2013). Polymer nanocomposite foams. *Journal of Materials Chemistry. A, Materials for Energy and Sustainability*, *1*(12), 3837-3850. http://dx.doi.org/10.1039/c2ta00086e.
10. Seraji, S. M., Aghjeh, M. K. R., Davari, M., Hosseini, M. S., & Khelgati, S. (2011). Effect of clay dispersion on the cell structure of LDPE/clay nanocomposite foams. *Polymer Composites*, *32*(7), 1095-1105. http://dx.doi.org/10.1002/pc.21127.
11. Anadao, P. (2014). *The use of montmorillonite clay in polymer nanocomposite foams*. In V. Mittal (Ed.), *Polymer nanocomposite foams* (pp. 149-168). Boca Raton: CRC Press.
12. Cui, Y., Kumar, S., Kona, B. R., & van Houcke, D. (2015). Gas barrier properties of polymer/clay nanocomposites. *RSC Advances*, *5*(78), 63669-63690. http://dx.doi.org/10.1039/C5RA10333A.
13. Azeredo, H. M. C. (2009). Nanocomposites for food packaging applications. *Food Research International*, *42*(9), 1240-1253. http://dx.doi.org/10.1016/j.foodres.2009.03.019.
14. Paul, D. R., & Robeson, L. M. (2008). Polymer nanotechnology: nanocomposites. *Polymer*, *49*(15), 3187-3204. http://dx.doi.org/10.1016/j.polymer.2008.04.017.

15. Majeed, K., Jawaid, M., Hassan, A., Bakar, A. A., Khalil, H. P. S. A., Salema, A. A., & Inuwa, I. (2013). Potential materials for food packaging from nanoclay/natural fibres filled hybrid composites. *Materials & Design*, *46*, 391-410. http://dx.doi.org/10.1016/j.matdes.2012.10.044.
16. Laguna-Gutierrez, E., Escudero, J., & Rodriguez-Perez, M. A. (2018). Analysis of the mechanical properties and effective diffusion coeficiente under static creep loading of low-density foams based on polyethylene/clays nanocomposites. *Composites. Part B, Engineering*, *148*, 156-165. http://dx.doi.org/10.1016/j.compositesb.2018.04.057.
17. Huitric, J., Ville, J., Mederic, P., & Aubry, T. (2017). Solid-state morphology, structure, and tensile properties of polyethylene/polyamide/nanoclay blends: effect of clay fraction. *Polymer Testing*, *58*, 96-103. http://dx.doi.org/10.1016/j.polymertesting.2016.12.020.
18. Liang, G., Xu, J., Bao, S., & Xu, W. (2004). Polyethylene/maleic anhydride grafted polyethylene/organic-montmorillonite nanocomposites. I. Preparation, microstructure, and mechanical properties. *Journal of Applied Polymer Science*, *91*(6), 3974-3980. http://dx.doi.org/10.1002/app.13612.
19. Siedenbiedel, F., & Tiller, J. C. (2012). Antimicrobial polymers in solution and on surfaces: overview and functional principles. *Polymers*, *4*(1), 46-71. http://dx.doi.org/10.3390/polym4010046.
20. Galli, R., Hall, M. C., Breitenbach, E. R., Colpani, G. L., Zanetti, M., Mello, J. M. M., Silva, L. L., & Fiori, M. A. (2020). Antibacterial polyethylene - ethylene vinyl acetate polymeric blend by incorporation of zinc oxide nanoparticles. *Polymer Testing*, *89*, 106554. http://dx.doi.org/10.1016/j.polymertesting.2020.106554.
21. Vilas, C., Mauricio-Iglesias, M., & García, M. (2020). Model-based design of smart active packaging systems with antimicrobial activity. *Food Packaging and Shelf Life*, *24*, 100446. http://dx.doi.org/10.1016/j.fpsl.2019.100446.
22. Zhong, Y., Godwin, P., Jin, Y., & Xiao, H. (2020). Biodegradable polymers and green based antimicrobial packaging materials: a mini-review. *Advanced Industrial and Engineering Polymer Research*, *3*(1), 27-35. http://dx.doi.org/10.1016/j.aiepr.2019.11.002.
23. Rojas, K., Canales, D., Amigo, N., Montoille, L., Cament, A., Rivas, L. M., Gil-Castell, O., Reyes, P., Ulloa, M. T., Ribes-Greus, A., & Zapata, P. A. (2019). Effective antimicrobial materials based on low-density polyethylene (LDPE) with zinc oxide (ZnO) nanoparticles. *Composites. Part B, Engineering*, *172*, 173-178. http://dx.doi.org/10.1016/j.compositesb.2019.05.054.
24. Li, S.-C., & Li, Y.-N. (2010). Mechanical and antibacterial properties of modified nano-ZnO/high density polyethylene composite films with a low doped content of nano-ZnO. *Journal of Applied Polymer Science*, *116*(5), 2965-2969. http://dx.doi.org/10.1002/app.31802.
25. Das-Gupta, D. K. (1994). Polyethylene: structure, morphology, molecular motion and dieletric behavior. *IEEE Electrical Insulation Magazine*, *10*(3), 5-15. http://dx.doi.org/10.1109/57.285418.
26. Paiva, L. B., Morales, A. R., & Días, F. R. V. (2008). Organoclays: properties, preparation and applications. *Applied Clay Science*, *42*(1-2), 8-24. http://dx.doi.org/10.1016/j.clay.2008.02.006.
27. Roy, A., Joshi, M., & Butola, B. S. (2019). Preparation and antimicrobial assessment of zinc-montmorillonite intercalates based HDPE nanocomposites: a cost-effective and safe bioactive plastic. *Journal of Cleaner Production*, *212*, 1518-1525. http://dx.doi.org/10.1016/j.jclepro.2018.11.235.
28. Coleman, M. M., Moskala, E. J., Painter, P. C., Walsh, D. J., & Rostami, S. (1983). A Fourier transform infra-red study of the phase behaviour of polymer blends. Ethylene-vinyl acetate copolymer blends with poly(vinyl chloride) and chlorinated polyethylene. *Polymer*, *24*(11), 1410-1414. http://dx.doi.org/10.1016/0032-3861(83)90221-5.
29. Gulmine, J. V., Janissek, P. R., Heise, H. M., & Akcelrud, L. (2002). Polyethylene characterization by FTIR. *Polymer Testing*, *21*(5), 557-563. http://dx.doi.org/10.1016/S0142-9418(01)00124-6.
30. Holešová, S., Samlíková, M., Ritz, M., & Pazdziora, E. (2015). Antibacterial polyethylene/clay nanocomposites using chlorhexidine as organic modifier. *Materials Today: Proceedings*, *2*(1), 246-252.
31. Terui, Y., & Hirokawa, K. (1994). Fourier transform infrared emission spectra of poly(vinyl acetate) enhanced by the island structure of gold. *Vibrational Spectroscopy*, *6*(3), 309-314. http://dx.doi.org/10.1016/0924-2031(93)E0065-A.
32. Yang, D., Yuan, P., Zhu, J. X., & He, H.-P. (2007). Synthesis and characterization of antibacterial compounds using montmorillonite and chlorhexidine acetate. *Journal of Thermal Analysisand Calorimery*, *89*(3), 847-852. http://dx.doi.org/10.1007/s10973-006-8318-3.
33. Zhao, C., Qin, H., Gong, F., Feng, M., Zhang, S., & Yang, M. (2005). Mechanical, thermal and flammability properties of polyethylene/clay nanocomposites. *Polymer Degradation & Stability*, *87*(1), 183-189. http://dx.doi.org/10.1016/j.polymdegradstab.2004.08.005.
34. Boronat, T., Fombuena, V., Garcia-Sanoguera, D., Sanchez-Nacher, L., & Balart, R. (2015). Development of a biocomposite based on green polyethylene biopolymer and eggshell. *Materials & Design*, *68*, 177-185. http://dx.doi.org/10.1016/j.matdes.2014.12.027.
35. Zhang, Q., Naito, K., Qi, B., & Kagawa, Y. (2009). Epoxy nanocomposites based on high temperature pyridinium-modified clays. *Journal of Nanoscience and Nanotechnology*, *9*(1), 209-215. http://dx.doi.org/10.1166/jnn.2009.J057. PMid:19441298.
36. Muñoz-Shugulí, C., Rodríguez, F. J., Bruna, J. E., Galotto, M. J., Sarantópoulos, C., Perez, M. A. F., & Padula, M. (2019). Cetylpyridinium bromide-modified montmorillonite as filler in low density polyethylene nanocomposite films. *Applied Clay Science*, *168*, 203-210. http://dx.doi.org/10.1016/j.clay.2018.10.020.
37. Lujan-Acosta, R., Sánchez-Valdes, S., Ramírez-Vargas, E., Ramos-DeValle, L. F., Espinoza-Martinez, A. B., Rodriguez-Fernandez, O. S., Lozano-Ramirez, T., & Lafleur, P. G. (2014). Effect of amino alcohol functionalized polyethylene as compatibilizer for LDPE/EVA/clay/flame-retardant nanocomposites. *Materials Chemistry and Physics*, *146*(3), 437-445. http://dx.doi.org/10.1016/j.matchemphys.2014.03.050.
38. Durmuş, A., Woo, M., Kaşgöz, A., Macosko, C. W., & Tsapatsis, M. (2007). Intercalated linear low density polyethylene (LLDPE)/clay nanocomposites prepared with oxidized polyethylene as a new type compatibilizer: structural, mechanical and barrier properties. *European Polymer Journal*, *43*(9), 3737-3749. http://dx.doi.org/10.1016/j.eurpolymj.2007.06.019.
39. Olewnik, E., Garman, K., & Czerwiński, W. (2010). Thermal properties of new composites based on nanoclay, polyethylene and polypropylene. *Journal of Thermal Analysis and Calorimetry*, *101*(1), 323-329. http://dx.doi.org/10.1007/s10973-010-0690-3.
40. Dadfar, S. M. A., Alemzadeh, I., Dadfar, S. M. R., & Vosoughi, M. (2011). Studies on the oxygen barrier and mechanical properties of low density polyethylene/organoclay nanocomposite films in the presence of ethylene vinyl acetate copolymer as a new type of compatibilizer. *Materials & Design*, *32*(4), 1806-1813. http://dx.doi.org/10.1016/j.matdes.2010.12.028.
41. Passador, F. R., Travain, D. R., Backes, E. H., Ruvolo, A. Fo., & Pessan, L. A. (2013). HDPE/LLDPE blend-based

nanocomposites – part II: evaluation of thermal, optical and transport properties. *Polímeros: Ciência e Tecnologia*, *23*(6), 748-757. http://dx.doi.org/10.4322/polimeros.2013.065.

42. Conceição, I. D., Silva, L. R. C., Carvalho, L. H., Costa, T. H. C., Silva, H. S., Alves, T. S., Barbosa, R., & Sousa, R. R. M. (2019). Evaluation of the effect of plasma treatment on the surface of green polyethylene and vermiculite clay films. *Matéria*, *24*(4), e-12492.
43. Almansoori, A., Majewski, C., & Rodenburg, C. (2017). Nanoclay/polymer composite powders for use in laser sintering applications: effects of nanoclay plasma treatment. *JOM*, *69*(11), 2278-2285. http://dx.doi.org/10.1007/s11837-017-2408-5. PMid:31983865.
44. Min, K. D., Kim, M. Y., Choi, K.-Y., Lee, J. H., & Lee, S.-G. (2006). Effect of layered silicates on the crystallinity and mechanical properties of HDPE/MMT nanocomposite blown films. *Polymer Bulletin*, *57*(1), 101-108. http://dx.doi.org/10.1007/s00289-006-0537-z.

Received: June 08, 2021
Revised: Apr. 14, 2022
Accepted: Aug. 18, 2022